micro

MDPI

Article

Polygalacturonic Acid Gels and Supramolecular Gels Loaded with a Drug, Bioceramics and Bioglass

Rebecca Sikkema [1] and Igor Zhitomirsky [2,*]

[1] School of Biomedical Engineering, McMaster University, Hamilton, ON L8S 4L8, Canada; sikkemar@mcmaster.ca
[2] Department of Materials Science and Engineering, McMaster University, Hamilton, ON L8S 4L8, Canada
* Correspondence: zhitom@mcmaster.ca

Abstract

This investigation addressed challenges in the delivery of poorly soluble drugs, and the colloidal processing of polymer–ceramic composites by fabrication of advanced supramolecular hydrogels. Polygalacturonic acid (PGA) polymer and 18β-glycyrrhetinic acid (GA) drug, both characterized by poor aqueous solubility, were selected as model building blocks for supramolecular hydrogels. Meglumine (MG) served as a multifunctional component in the gels, acting as a building block as well as an alkalizing and solubilizing agent for PGA and GA. Investigations revealed gel formation mechanisms, which were based on the electrostatic interactions of deprotonated anionic carboxylic groups of PGA and GA with protonated amino groups of MG and the hydrogen bonding of PGA polymer and GA molecules. The feasibility of the fabrication of PGA-MG and GA-MG gels opened an avenue for the fabrication of PGA-GA-MG gels. The composite gels provided a platform for drug delivery, and the kinetics of drug release from the composite gels containing MG excipient were investigated. Composite gels were obtained from colloidal dispersions, containing bioceramics, such as hydroxyapatite, silica, and titania, and bioglass in the PGA solutions in the presence of MG. The results of this investigation pave the way for the fabrication of novel supramolecular and composite gels loaded with various functional materials.

Keywords: polygalacturonic acid; supramolecular gel; hydroxyapatite; meglumine; titania; silica; bioglass; hydrogel; drug

Check for updates

Academic Editors: José Agustín Tapia Hernández, Carlos Gregorio Barreras-Urbina and Francisco Rodríguez-Félix

Received: 8 April 2026
Revised: 18 May 2026
Accepted: 25 May 2026
Published: 2 June 2026

Copyright: © 2026 by the authors. Licensee MDPI, Basel, Switzerland. This article is an open access article distributed under the terms and conditions of the Creative Commons Attribution (CC BY) license.

1. Introduction

Hydrogels have been a widely researched area of study for applications in biomedicine, agriculture, hygiene, energy storage and environmental engineering [1,2]. Hydrogels can be prepared in various forms, such as coatings, thin films, fibers, slabs, and porous implants of different shapes. The highly tunable properties of hydrogels, such as water content, porosity, mechanical strength, and biodegradability, make them exceptionally versatile across a wide range of applications [1,2]. Various gel formation strategies, such as chemical crosslinking and supramolecular gel assembly, have been employed to manipulate gel properties for the desired application.

Chemical crosslinking strategies have been employed with both covalent and ion-based crosslinking. Crosslinking strategies include applications of disulfide [3], short chain hyaluronate [4], and glycidylmethacrylate [5]. Ionic crosslinking strategies have been employed with ions such as La, Ca, Al, Cu, Fe, and Zn [6,7], usually requiring an increase in pH for crosslinking and gelation to occur. Gel strength was seen to increase as the cation

saturation increased. A combination of conformational changes in the polymer chain as well as electrostatic interactions between the cations and the negatively charged carboxylate groups have been shown to induce the gelation effect. Gelation occurs in a two-step process: first, the formation of strong dimer associations, followed by weaker electrostatic interactions [6]. Some challenges have been seen through the use of cation crosslinkers, such as tissue calcification due to the presence of metal ions [4]. Researchers have found that covalent crosslinking demonstrates good drug release properties, in particular due to ionic washout or ion exchange in systems, where the external ion concentration is lower than that in the gel, thereby disrupting the gel network and causing more rapid drug release [5].

Supramolecular gels represent another important class of hydrogels. Supramolecular gels, with their ability to respond to external stimuli, offer exceptional potential for advanced applications [8]. Supramolecular gel structures are stabilized by electrostatic, hydrogen bonding, Van der Waals and π–π interactions [9]. Supramolecular gels have generated significant interest for drug delivery [10] and other biomedical applications [11]. With their unique structural and functional properties, supramolecular gels offer compelling potential for advanced energy storage systems, particularly as active materials in electrodes, binders, and electrolytes [12]. Due to their dynamic and reversible nature, supramolecular gels provide advantages across a wide range of applications in which the rigidity of chemically crosslinked gels leads to significant challenges and limitations [13–15]. Such applications involve minimally invasive procedures of drug or protein injection, 3D printing, dental and surgical filling, and wound healing [16–18]. The advances in the development of supramolecular gels have generated interest in the development of new building blocks for their fabrication.

Polygalacturonic acid (PGA) is a promising building block for supramolecular gel fabrication. PGA is a natural polysaccharide produced from pectin degradation. Its application in the biomedical industry is widespread, as it is a non-toxic, biodegradable, antibacterial, antiadhesive, and highly biocompatible material for many applications [19–22]. PGA has applications in biosensors [5,23], tissue engineering, and bone repair due to its support of cell adhesion and proliferation [24,25]. The addition of ceramic particles to PGA gels has been seen to increase the mechanical properties of the gels due to ceramic–polymer interactions increasing polymer chain density in the gel, leading to a beneficial environment for bone repair [26]. Many applications are focused on drug delivery in various systems [3,27,28]. PGA gels have been used for in vivo drug release to suppress inflammatory responses [27]. The release of rosmarinic acid from PGA gels has been seen to reduce postsurgical adhesion [3]. These studies highlight PGA as a highly promising candidate for gel formation.

The goal of this investigation was the fabrication of supramolecular PGA gels loaded with different functional materials. The feasibility of preparation of PGA–meglumine (MG) gels was demonstrated. It was found that MG facilitated the solubilization of PGA in aqueous solutions. The mechanism of gel formation involved ion-pair formation, which facilitated gelation. The interest in the use of the FDA-approved MG alkalizer was motivated by its wide applications for solubilization of various drugs and drug delivery [10]. It was found that the poorly soluble 18ß-glycyrrhetinic acid (GA) drug can also be dissolved in the presence of MG. In this investigation, GA was applied as a model drug material, which has generated interest for various biomedical applications due to its anti-inflammatory effect [29], antioxidant properties [30] and antitumor effect [31]. Another important finding was the feasibility of the fabrication of GA-MG supramolecular gels. Such findings provided a platform for the fabrication of composite PGA-GA-MG gels. Moreover, various bioceramics, such as hydroxyapatite, titania, silica and bioglass, were dispersed in PGA-

MG solutions, and composite PGA-MG gels loaded with bioceramics and bioglass were prepared. The composite gels provide a platform for controlled drug delivery, and the drug release rate was investigated. It was demonstrated that the results of this investigation open an avenue for the fabrication of novel polymer and supramolecular gels, loaded with various functional biomaterials.

2. Materials and Methods

Polygalacturonic acid (PGA), meglumine (MG), 18ß-glycyrrhetinic acid (GA), TiO_2 (average particle size of 21 nm), calcium nitrate tetrahydrate, ammonium phosphate dibasic, and ammonium hydroxide were purchased from MilliporeSigma (Oakville, ON, Canada). Amorphous silica (average particle size of 0.5 µm) was purchased from PCR Inc. (Gainesville, FL, USA). Hydroxyapatite (HA) nanoparticles were synthesized by chemical precipitation [32] from calcium nitrate tetrahydrate and ammonium phosphate dibasic by using a stochiometric 5:3 molar ratio of Ca:P and a solution pH of 11 through the use of ammonium hydroxide. Bioactive glass powder (45S5 Bioglass®) of composition (wt%) 45% SiO_2, 24.5% Na_2O, 24.5% CaO and 6% P_2O_5 and an average particle size < 5 µm (Mo Sci corporation, Rolla, MO, USA) was used.

PGA- and GA-based gels were formed by mixing PGA polymer and MG in a 1:1 molar ratio of PGA monomer to MG and a 1:1 molar ratio of GA to MG in aqueous solutions at room temperature. Excess water was removed through drying under ambient conditions. Composite drug-loaded gels were prepared using a 1:1:2 molar ratio of PGA, GA, and MG, following the same protocol as that used for the individual gel formulations. Bioceramic functionalization of the gels used the base PGA gel preparation procedure with the addition of a 1:1 mass ratio of PGA to a bioceramic, either hydroxyapatite, titania, silica, or bioglass. In this procedure, the PGA solutions prepared using MG and containing bioceramics or bioglass were ultrasonicated in a bath to improve particle dispersion prior to gel formation. Concentrations for gel fabrication ranged from 50 to 300 g L^{-1} PGA for PGA-based gels and from 50 to 200 g L^{-1} GA for the GA-MG gel, all of which were solubilized in 10–30 mL of DI water. The gels had a starting pH of 9. Higher solution concentrations lead to more rapid gelation. The gels were stored in ambient conditions.

The gel composition was characterized by X-ray diffraction using a Bruker D8 Venture powder diffractometer (Madison, WI, USA) with monochromatized CuKα radiation and FTIR using a Bruker Vertex 70 spectrometer (Milton, ON, Canada). The gels were dried and coated with 3 nm Pt to assess the gel morphology using an FEI Magellan 400 scanning electron microscopy (SEM) instrument (Hillsboro, OR, USA). The PGA-MG gel and bioceramic- or bioglass-based gels underwent thermogravimetric analysis on a Netzsch STA 409 instrument (Exton, PA, USA) at a heating rate of 5 °C min^{-1} in air atmosphere.

Gel swelling studies were conducted by weighing the gels at the point where the excess water had evaporated, leading to a solid gel, followed by weighing the samples upon complete drying in a desiccator. The swelling ratio (S) was calculated as [33]

$$S(\%) = \frac{M_i - M_d}{M_d} \times 100 \quad (1)$$

where M_i is the initial mass of the gels and M_d is the mass of the dried gels.

Drug release from PGA-GA-MG gels was performed. Three cylindrically shaped gel samples (gel mass of ~0.5 g and GA mass of ~0.2 g) were each placed in 7 mL of phosphate-buffered saline (PBS) at room temperature. At set timepoints, the PBS solution was fully removed and replaced with fresh PBS. The drug concentration was measured in the removed solution by UV spectrophotometry using a Tecan Infinite M200 Pro plate

reader (Morrisville, NC, USA) and Tecan i-control software version 3.37 in absorbance mode at 252 nm.

3. Results

Figure 1 shows the chemical structures of PGA, MG and GA. PGA is a natural carbohydrate polymer material. The chemical structure of PGA (Figure 1A) contains OH and carboxylic groups. PGA was used in its water-insoluble acidic form, containing protonated carboxylic groups. MG (Figure 1B) is a carbohydrate derivative of sorbitol in which one OH group is substituted with a methylamino (NH–CH_3) group [34]. The large number of OH groups plays a key role in promoting the MG's pronounced water solubility [35]. Protonation of the NH group in MG promotes the generation of basic solutions [35]. GA is a pentacyclic triterpenoid characterized by its hydrophobic nature, poor water solubility, and the presence of the protonated COOH group (Figure 1C).

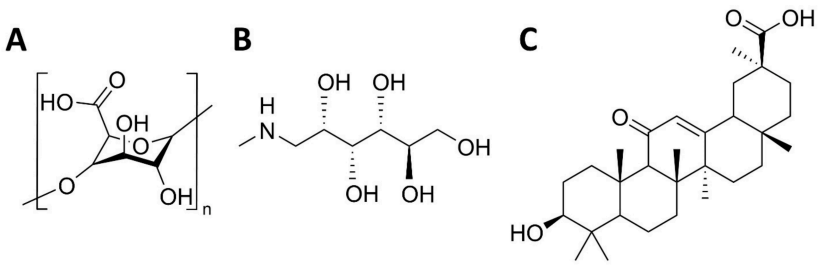


Figure 1. Chemical structures of (**A**) PGA, (**B**) MG and (**C**) GA.

This PGA was dissolved in water in the presence of MG to form basic solutions. In such solutions, the COOH groups of PGA were deprotonated, and electrostatic repulsion of the anionic deprotonated molecules facilitated their dissolution. The drying of the obtained solutions resulted in the formation of PGA-MG supramolecular gels (Figure 2A). The gelling time decreased with the increase in the concentration of MG and PGA. For 300 g L^{-1} PGA, the process was completed in 3 h. Figure 2B compares the TGA and DTA data for as-received PGA and PGA-MG gel. The mass loss was attributed to the burning-out of the organic materials. However, the complete burning-out of PGA-MG gel was observed at higher temperatures, compared with PGA. The TGA curve of the PGA-MG gel showed an additional step in the range of 400–600 °C. The DTA data showed endothermic peaks below ~160 °C related to dehydration and exothermic peaks related to the burning-out of the organic materials. However, the endothermal and exothermal effects for the PGA-MG gels were shifted to higher temperatures, compared with PGA. The difference in the thermal behavior of PGA-MG gels and as-received PGA polymer can be attributed to PGA-MG interactions.

Figure 2C,D present the SEM images of PGA-MG gels at different magnifications. The SEM images show a continuous and crack-free morphology. The XRD pattern of as-received MG shows peaks corresponding to JCPDS 02-070-8267 (Figure 2E). The diffraction pattern of PGA shows two broad peaks centered at ~13 and 22.5 degrees. The diffraction peaks of MG and PGA were not observed in the diffraction pattern of PGA-MG gel, which showed two very broad peaks centered at ~8 and ~21 degrees. Therefore, the obtained gel cannot be considered a mixture of MG and PGA. It is suggested that the acid–amine gelation mechanism [36] was involved in gel formation. It is based on ion-pair formation and electrostatic interactions of the positively charged protonated NH_2^+ group of MG and negatively charged COO^- groups of PGA (Figure 3). Moreover, similar to other gels [36], the interaction of OH groups of MG and PGA resulted in hydrogen bond formation (Figure 3).

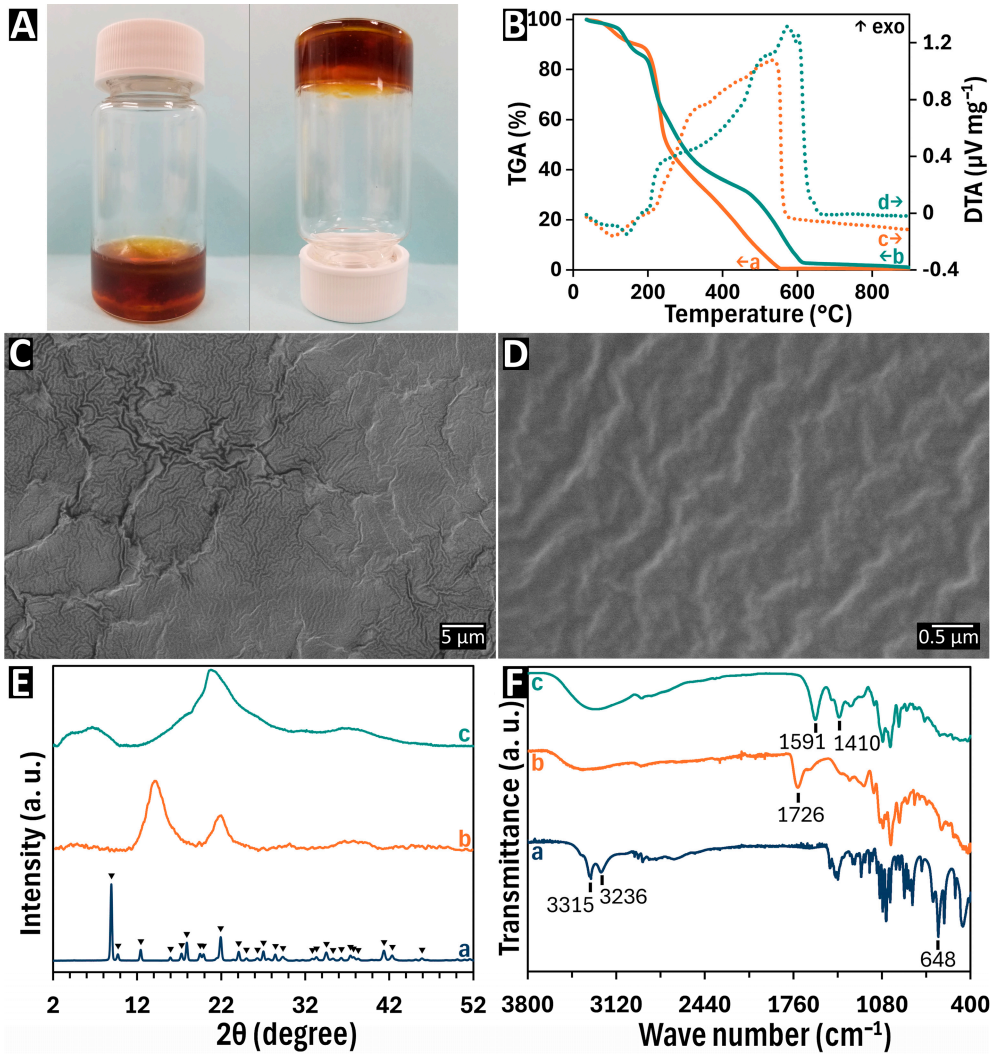


Figure 2. (**A**) PGA-MG gel. (**B**) (a,b) TGA and (c,d) DTA data for (a,c) as-received PGA and (b,d) PGA-MG gel. (**C**,**D**) SEM images of PGA-MG gel at different magnifications. (**E**) XRD and (**F**) FTIR data for (a) MG, where ▼—peaks corresponding to JCPDS file 02-070-8267; (b) PGA; and (c) PGA-MG gel.

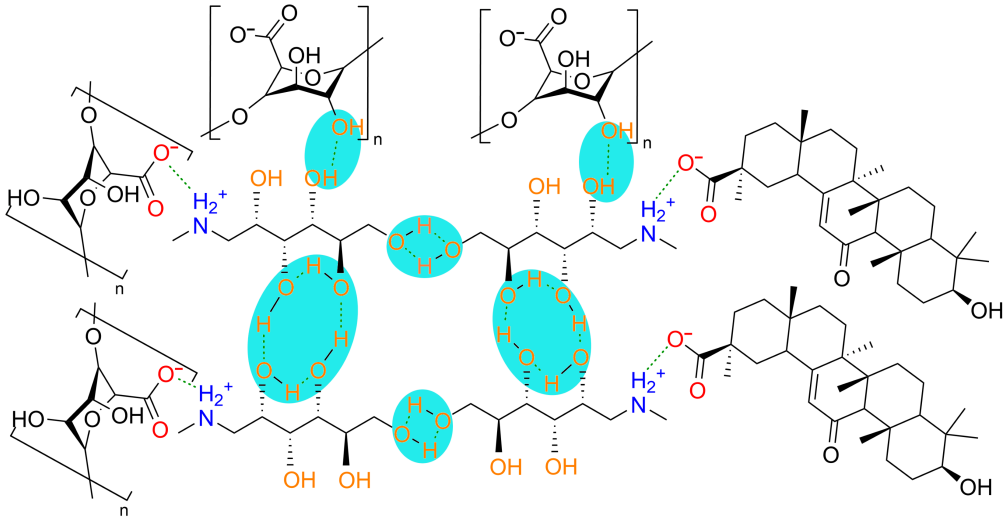


Figure 3. Hydrogen bonding (highlighted) and electrostatic interactions of deprotonated PGA and GA with protonated MG in the gels.

FTIR data confirmed that carboxylic groups in the gel were deprotonated. Figure 2F compares FTIR data for as-received MG, as-received PGA and the obtained PGA-MG gel. The FTIR spectrum of MG corresponds to the literature data [37]. It presents peaks corresponding to C—O stretching, O—H bending, N—H stretching and O—H stretching at 1048, 1239, 3235 and 3314 cm^{-1}, respectively. The multiple peaks centered at 648 cm^{-1} are related to out-of-plane O—H bending vibrations. The spectrum of as-received PGA shows a peak at 1726 cm^{-1} due to C=O stretching, which was not observed in the spectrum of PGA-MG gel. However, the spectrum of the gel showed peaks at 1591 and 1410 cm^{-1}, which are related to asymmetric and symmetric stretching vibrations of the deprotonated carboxylic group [38], respectively. Therefore, PGA was in its deprotonated form in the PGA-MG gel. The absorption related to the N—H stretching of MG was not observed in the spectrum of the PGA-MG gel due to protonation of the amino group. The protonation of NH groups can result in peak shifting to much lower wavenumbers and broadening or peak disappearing. The absorption related to O—H stretching and bending vibrations observed in the spectrum of MG was not observed in the spectrum of PGA-MG gels. This can be attributed to the hydrogen bonding of MG and PGA molecules, which can suppress the O—H stretching and bending vibrations in the disordered and hydrated hydrogel structure. Figure 3 shows the suggested gelation mechanism, which involves electrostatic interactions of deprotonated carboxylic groups of PGA and protonated NH groups of MG. Figure 3 also illustrates hydrogen bonding interaction of MG molecules and hydrogen bonding interactions of PGA and MG. Moreover, it is known [39] that hydrogen bonding between PGA molecules can facilitate gel formation. Hydrogen bonding interactions are also influenced by adsorbed water. The comparison of the PGA-MG dried gel mass with the mass of the PGA and MG materials used for gel preparation showed that water content in the gel was 42% and the swelling ratio was 74%.

MG was also used for the solubilization of GA and formation of GA-MG supramolecular gels (Figure 4A). The gelling time decreased with the increase in concentration of GA and MG. For 200 g L^{-1} GA, the process was completed in 2 h. SEM investigations of the gels showed a continuous crack-free morphology (Figure 4B). It is suggested that the mechanism of GA-MG gel formation is similar to that of PGA-MG. It involved the deprotonation of the COOH group of GA and solubilization of the GA molecules. The electrostatic interactions of the negatively charged deprotonated GA molecules with positively charged protonated MG (Figure 3) and the hydrogen bonding of MG molecules facilitated the formation of the supramolecular gels. The ability to form PGA-MG and GA-MG gels opened an avenue for the fabrication of composite PGA-GA-MG gels (Figure 4C). The SEM studies of such gels showed a relatively rough surface (Figure 4D) with small surface microcracks. The GA-MG and PGA-GA-MG gels were studied by XRD and FTIR methods. The diffraction pattern of as-received GA showed its crystallinity in agreement with other published XRD data [40,41] for this material. The XRD peaks of GA and MG were not observed in diffraction patterns of GA-MG and PGA-GA-MG gels. Therefore, the GA-MG and PGA-GA-MG materials cannot be considered mixtures of the individual crystals. The XRD patterns of GA-MG and PGA-GA-MG showed very broad peaks centered at diffraction angles of ~4 and ~14 degrees.

The FTIR spectrum of GA showed absorption at 1703 and 1662 cm^{-1}, which can be related to C=O stretching vibrations. Turning again to the chemical structure of GA presented in Figure 1C, it is seen that GA has two C=O groups, representing segments of carboxylic and ketone ligands. Both groups can contribute to gel formation by electrostatic interactions or hydrogen bonding. The deprotonation of the carboxylic group can result in electrostatic interactions of PGA and GA with MG (Figure 3). Moreover, the C=O group of the ketone ligands can contribute to hydrogen bonding by interactions with NH or OH groups of

MG [42]. The GA peaks at 1703 and 1662 cm^{-1} were not observed in the FTIR spectrum of the GA-MG and PGA-GA-MG gels. The FTIR spectrum of GA-MG gel shows absorption at 1639 and 1391 cm^{-1}. The FTIR spectrum of PGA-MGA-MG showed absorption at 1639 and 1389 cm^{-1} Such absorption can result from asymmetric and symmetric stretching vibrations of the deprotonated carboxylic group. FTIR analysis shows that the carboxylic groups of PGA and GA are deprotonated and that the C=O group participates in hydrogen bonding, leading to the disappearance of its corresponding absorption band. Moreover, the absorption associated with the stretching and bending vibrations of the OH groups in MG was absent in the gel spectra, indicating their involvement in hydrogen bonding.

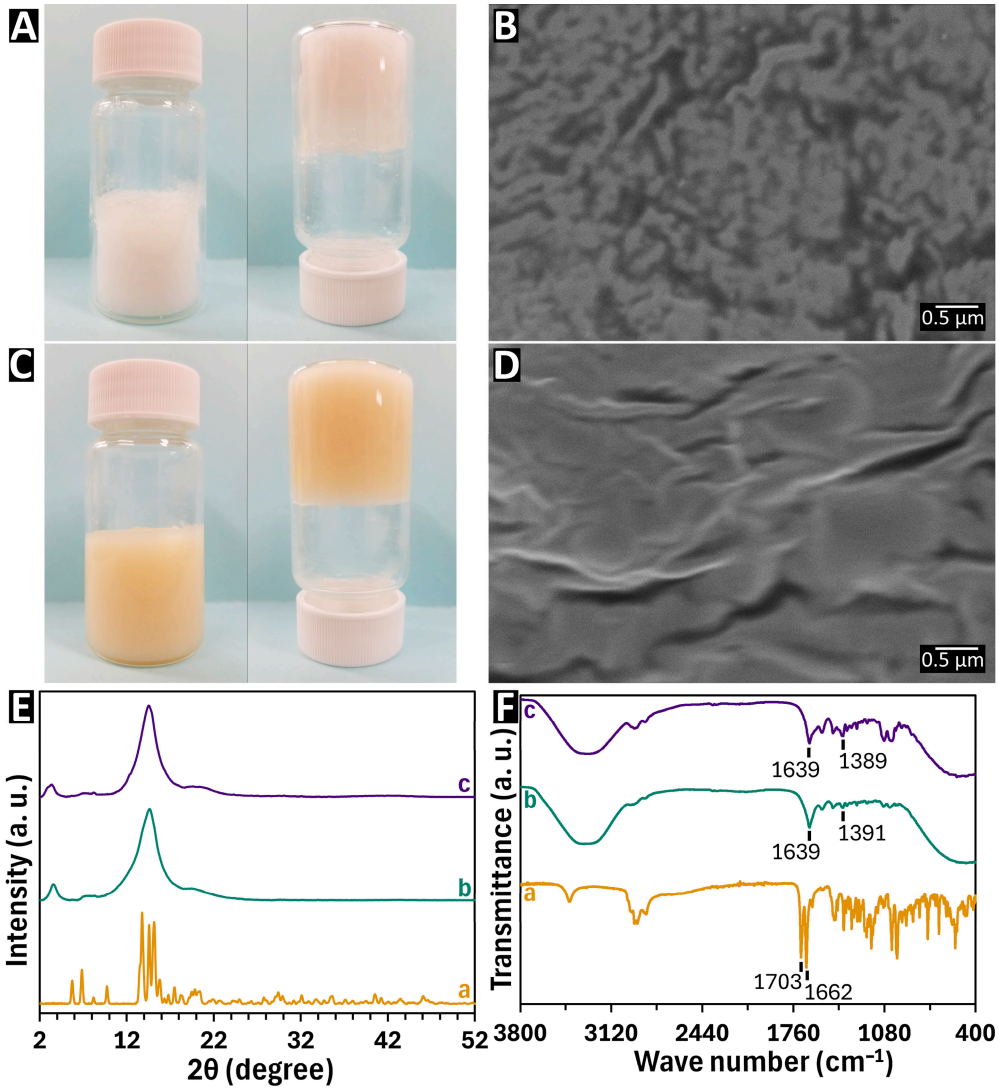


Figure 4. (**A**) GA-MG gel. (**B**) SEM image of GA-MG gel. (**C**) PGA-GA-MG gel. (**D**) SEM image of PGA-GA-MG gel. (**E**) XRD and (**F**) FTIR data for (a) as-received GA, (b) GA-MG gel and (c) PGA-GA-MG gel.

The water contents in the GA-MG and PGA-GA-MG gels were found to be 72 and 75%, respectively, with swelling ratios of 260 and 294% for GA-MG and PGA-GA-MG gels, respectively. Therefore, hydrogen bonding involved absorbed water molecules. Figure 5 shows the kinetics of GA drug release from the PGA-GA-MG gel, with the calibration curve shown in the Supplementary Information (Figure S1). The composite gels exhibited a sustained drug release profile, suggesting their potential for controlled delivery. It is important to note that the kinetics of GA release can be influenced by gel composition.

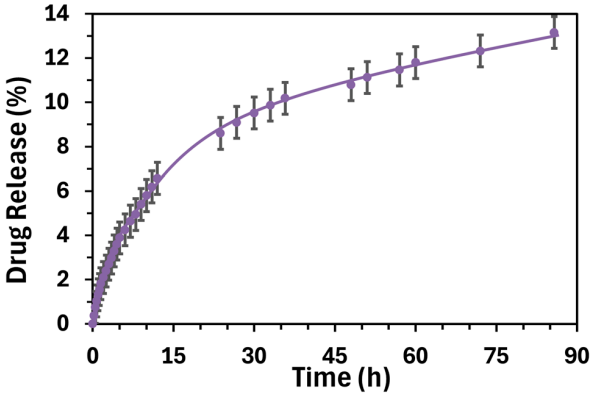


Figure 5. Kinetics of GA drug release from the PGA-GA-MG gel.

In this investigation, composite gels containing bioceramics and bioglass were also obtained. The use of PGA instead of sodium salt of PGA offered benefits of improved purity and better suspension stability, which is usually reduced in the presence of Na ions [24]. Figure 6A shows gels containing hydroxyapatite, silica, titania, and bioglass. PGA-MG-HA, PGA-MG-SiO_2, PGA-MG-TiO_2, and PGA-MG–bioglass gels contained 43, 40, 52 and 55% of water, respectively. The swelling ratios of these gels were 75, 68, 106, and 125% for the PGA-MG-HA, PGA-MG-SiO_2, PGA-MG-TiO_2, and PGA-MG–bioglass gels, respectively. The effect of inorganic particles on hydrogel swelling can result from altering the network density and structural stability, introducing additional hydrophilic groups, steric hindrance effect, creation of micro-voids, Donnan osmotic effect and other factors [43–45]. The SEM images of the PGA-MG-based gels containing bioceramics and bioglass are presented in Figure 6B–E. The SEM images show ceramic or bioglass particles in the gel matrix.

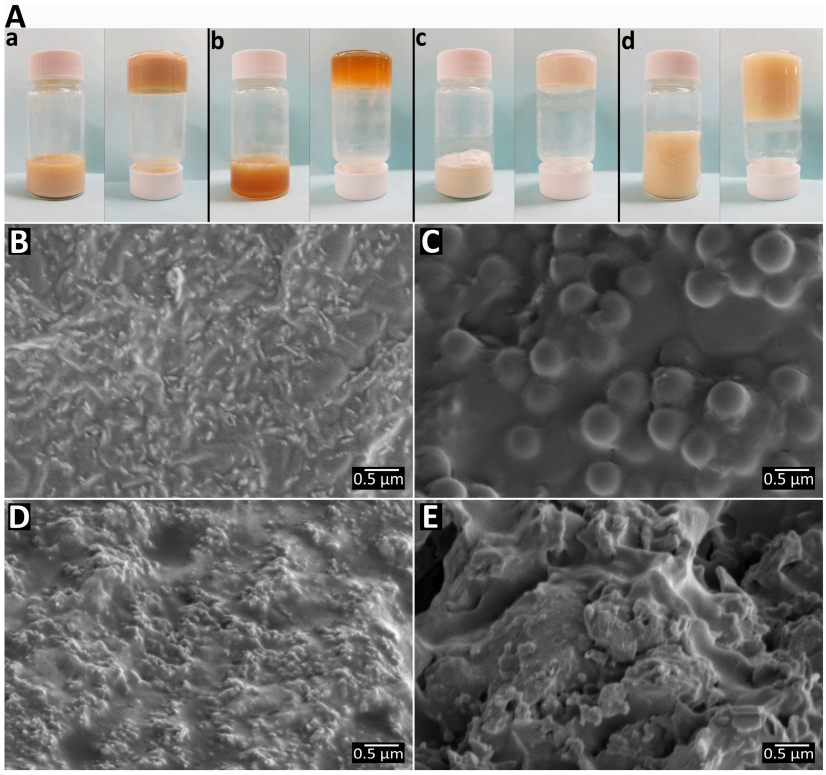


Figure 6. (**A**) (a) PGA-MG-HA gel, (b) PGA-MG-SiO_2 gel, (c) PGA-MG-TiO_2 gel, and (d) PGA-MG–bioglass gel and corresponding SEM images of (**B**) PGA-MG-HA, (**C**) PGA-MG-SiO_2, (**D**) PGA-MG-TiO_2 and (**E**) PGA-MG–bioglass gels.

It is important to note that swelling exerts significant influence on drug release in regular chemical gels, such as chemically crosslinked polymers, as well as in supramolecular gels. Regular chemical gels containing permanent chemical bonds of crosslinked polymers represent a sturdy cage, which can stretch extensively without breaking. Such gelling is irreversible, and the gel networks can be loaded with drugs and other materials. Regular chemical gels usually show significant swelling, which facilitates drug release from their structure. There is a strong link between the swelling of such gels and drug release. In contrast to regular crosslinked gels, supramolecular gels are formed by weak hydrogen bonds. Such bonds are dynamic and reversible; they can break and reform. The supramolecular gels studied in this work contain a drug as a component of their GA-MG gel structure. MG facilitates drug dissolution. In supramolecular gels, drug release is governed not only by swelling but also by slow solubilization of the drug in the presence of MG, which acts as a drug excipient.

HA and TiO_2 showed high crystallinity, and the formation of composite PGA-MG-HA and PGA-MG–TiO_2 gels was also confirmed by XRD (Figure 7A). The diffraction patterns of the composite gels show peaks of HA and TiO_2.

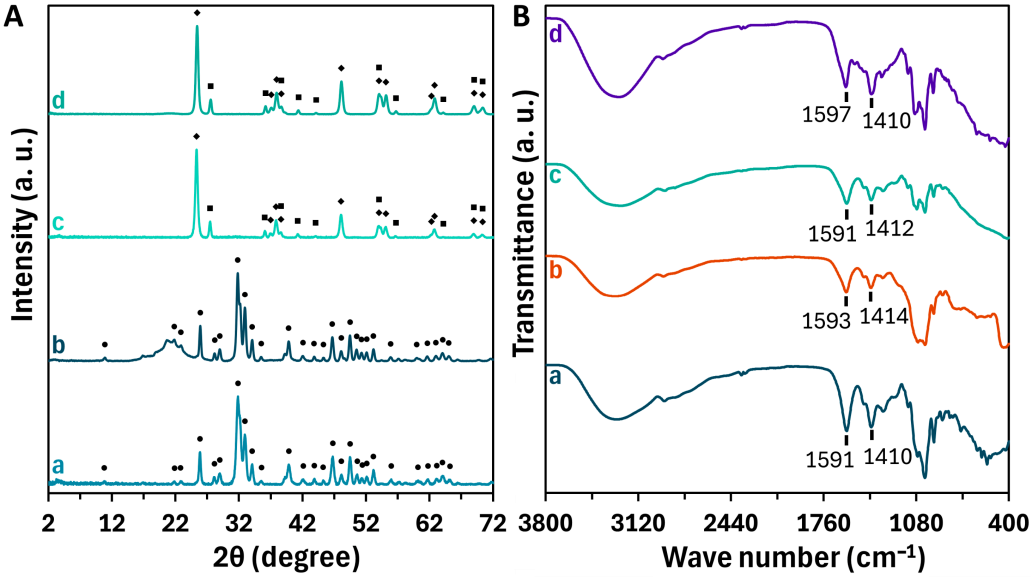


Figure 7. (**A**) XRD data for (a) as-prepared HA (•—peaks corresponding to JCPDS file 01-086-0740), (b) PGA-MG-HA gel, (c) as-received TiO_2 (♦—peaks corresponding to JCPDS file 00-021-1272 of anatase; ■—peaks corresponding to JCPDS file 01-086-4330 of rutile), and (d) PGA-MG-TiO_2 gel. (**B**) FTIR data for (a) PGA-MG-HA (b) PGA-MG-SiO_2, (c) PGA-MG-TiO_2, and (d) PGA-MG–bioglass gels.

The FTIR spectra (Figure 7B) showed absorption of deprotonated COOH groups of PGA in the ranges of 1591–1597 and 1410–1414 cm^{-1}, corresponding to asymmetric and symmetric vibrations, respectively. Similar absorption was observed for the pure PGA-MG gel (Figure 4F(b)). TGA data for the gels (Figure 8) showed several steps in mass loss related to the dehydration and burning-out of the organic components. However, in contrast to pure PGA-MG gel, which burned out completely below 550 °C, the composite gel showed remaining mass loss at 900 °C related to the dehydrated ceramic or glass phases.

The DTA curves showed broad endotherms at about 100 °C, which corresponded to the steps in mass loss. This endotherm can be related to dehydration of organic and inorganic components. It should be noted that mass loss related to dehydration can also be expected at higher temperatures. All the composite gels showed strong exotherms, related to the burning-out of the organic components. It should be noted that kinetics of the burning-out of the organic phase can be influenced by the inorganic phase, which can interact with the

organic phases and influence the diffusion of O_2 as well as diffusion of products of the oxidation reactions. The crystallization of bioglass can explain additional exothermic peaks in the DTA curve. Data from rheology studies presented in frequency dependencies of storage modulus G′ and loss modulus G″ reveal their frequency dependence, indicating the dynamic nature of supramolecular gels (Figure S2). Such behavior is frequently observed in various supramolecular gels [46–48], where network responds elastically only at short timescales. For PGA-MG, GA-MG, PGA-MG-HA, PGA-MG-TiO_2, and PGA-MG–bioglass gels, the larger G′ compared with G″ indicated relatively stable gel networks. For PGA-MG–bioglass gels the variation in G′ with frequency was relatively small, and G′ was significantly larger than G″, indicating improved stability of the gel network.

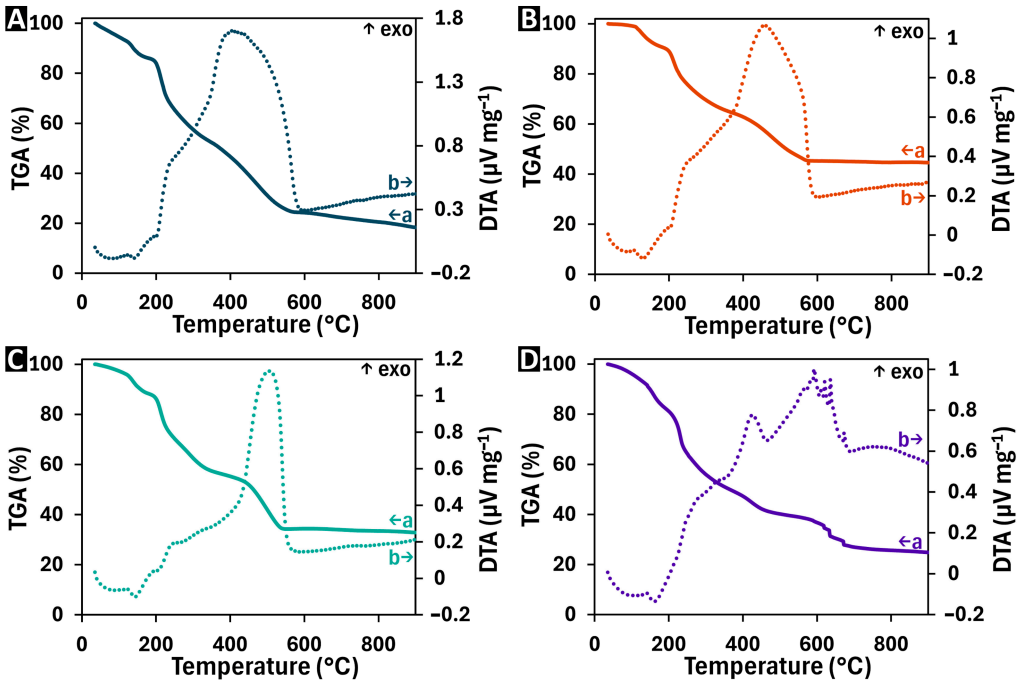


Figure 8. (a) TGA and (b) DTA data for (**A**) PGA-MG-HA, (**B**) PGA-MG-SiO_2, (**C**) PGA-MG-TiO_2, (**D**) PGA-MG–bioglass gels.

4. Conclusions

The successful preparation of PGA-MG and GA-MG supramolecular gels was demonstrated. MG functioned as a multifunctional molecule, acting as a building block in the supramolecular gel as well as an alkalizing and solubilizing agent for PGA and GA. The fabrication of PGA-MG and GA-MG gels was confirmed by XRD, TGA, DTA, and FTIR studies. Test results indicate that carboxylic groups of PGA and GA in the gels were deprotonated, and gel formation involved electrostatic interactions of the deprotonated carboxylic groups of PGA and GA with protonated groups of MG and hydrogen bonding interactions. The fabrication of PGA-MG and GA-MG gels provided a platform for the fabrication of composite PGA-GA-MG gels, which showed potential for controlled drug release due to the use of MG as excipient. It was found that PGA-MG gels can be loaded with HA, SiO_2, and TiO_2 bioceramics, and bioglass. The results of this investigation open up an avenue for the fabrication of novel supramolecular gels loaded with other functional materials.

Supplementary Materials: The following supporting information can be downloaded at: https://www.mdpi.com/article/10.3390/micro6020041/s1, Figure S1: Calibration curve of PGA-GA-MG gel drug release. Most drug concentrations measured fall within the 0–0.05 g L^{-1} range; Figure S2: G′

and G″ for gels of (A) PGA-MG, (B) GA-MG, (C) PGA-GA-MG, (D) PGA-MG-HA, (E) PGA-MG-SiO_2, (F) PGA-MG-TiO_2, and (G) PGA-MG–bioglass. Rheology studies were performed on TA Instruments Discovery HR-2 Hybrid Rheometer at room temperature under oscillatory shear.

Author Contributions: Conceptualization, R.S. and I.Z.; methodology, R.S.; validation, R.S., formal analysis, R.S.; investigation, R.S.; resources, I.Z.; data curation, R.S.; writing—original draft preparation, R.S.; writing—review and editing, R.S. and I.Z.; supervision, I.Z.; project administration, I.Z.; funding acquisition, I.Z. All authors have read and agreed to the published version of the manuscript.

Funding: This research study was funded by the Natural Sciences and Engineering Research Council of Canada, grant RGPIN-2024-03968 and the CRC program.

Institutional Review Board Statement: Not applicable.

Informed Consent Statement: Not applicable.

Data Availability Statement: The data are available in this manuscript.

Conflicts of Interest: The authors declare no conflicts of interest.

Abbreviations

The following abbreviations are used in this manuscript:

PGA	Polygalacturonic acid
MG	Meglumine
GA	18β-glycyrrhetinic acid
TGA	Thermogravimetric analysis
DTA	Differential thermal analysis
HA	Hydroxyapatite
XRD	X-ray diffraction
FTIR	Fourier transform infrared spectroscopy
SEM	Scanning electron microscopy

References

1. Hoffman, A.S. Hydrogels for biomedical applications. *Adv. Drug Deliv. Rev.* **2012**, *64*, 18–23. [CrossRef]
2. Chai, Q.; Jiao, Y.; Yu, X. Hydrogels for Biomedical Applications: Their Characteristics and the Mechanisms behind Them. *Gels* **2017**, *3*, 6. [CrossRef]
3. Peng, H.-H.; Chen, Y.-M.; Lee, C.-I.; Lee, M.-W. Synthesis of a disulfide cross-linked polygalacturonic acid hydrogel for biomedical applications. *J. Mater. Sci. Mater. Med.* **2013**, *24*, 1375–1382. [CrossRef] [PubMed]
4. Peng, H.-H.; Chen, J.-W.; Yang, T.-P.; Kuo, C.-F.; Wang, Y.-J.; Lee, M.-W. Polygalacturonic acid hydrogel with short-chain hyaluronate cross-linker to prevent postoperative adhesion. *J. Bioact. Compat. Polym.* **2011**, *26*, 552–564. [CrossRef]
5. Schneider, K.P.; Rollett, A.; Wehrschuetz-Sigl, E.; Hasmann, A.; Zankel, A.; Muehlebach, A.; Kaufmann, F.; Guebitz, G.M. Bioresponsive systems based on polygalacturonate containing hydrogels. *Enzym. Microb. Technol.* **2011**, *48*, 312–318. [CrossRef]
6. McKenna, B.A.; Nicholson, T.M.; Wehr, J.B.; Menzies, N.W. Effects of Ca, Cu, Al and La on pectin gel strength: Implications for plant cell walls. *Carbohydr. Res.* **2010**, *345*, 1174–1179. [CrossRef]
7. Yang, X.; Nisar, T.; Liang, D.; Hou, Y.; Sun, L.; Guo, Y. Low methoxyl pectin gelation under alkaline conditions and its rheological properties: Using NaOH as a pH regulator. *Food Hydrocoll.* **2018**, *79*, 560–571. [CrossRef]
8. Zheng, H.; Pochan, D. Spiers Memorial Lecture: Recent advances (and challenges) in supramolecular gels. *Faraday Discuss.* **2025**, *260*, 9–34. [CrossRef] [PubMed]
9. Mukai, M.; Kogiso, M.; Aoyagi, M.; Asakawa, M.; Shimizu, T.; Minamikawa, H. Supramolecular nanofiber formation from commercially available arginine and a bola-type diacetylenic diacid via hydrogelation. *Polym. J.* **2012**, *44*, 646–650. [CrossRef]
10. Zhang, C.; Sikkema, R.; Shi, C.; Tang, D.; Shi, K.; Zhitomirsky, I. New horizons in synthesis, functionalization, and deposition of advanced materials using multifunctional organic alkalizers. *Adv. Colloid Interface Sci.* **2025**, *346*, 103666. [CrossRef]
11. Ferreira, L.M.; Kurokawa, S.S.; Alonso, J.D.; Cassimiro, D.L.; Souza, A.L.R.d.; Fonseca, M.; Sarmento, V.H.V.; Regasini, L.O.; Ribeiro, C.A. Structural and thermal behavior of meglumine-based supra-amphiphiles in bulk and assembled in water. *Langmuir* **2016**, *32*, 11878–11887. [CrossRef] [PubMed]
12. Suja, S.K.; Mathiya, S. Supramolecular gels as materials for energy storage devices. *Next Mater.* **2025**, *8*, 100535. [CrossRef]

13. Chen, M.H.; Chung, J.J.; Mealy, J.E.; Zaman, S.; Li, E.C.; Arisi, M.F.; Atluri, P.; Burdick, J.A. Injectable supramolecular hydrogel/microgel composites for therapeutic delivery. *Macromol. Biosci.* **2019**, *19*, 1800248. [CrossRef]
14. Saunders, L.; Ma, P.X. Self-healing supramolecular hydrogels for tissue engineering applications. *Macromol. Biosci.* **2019**, *19*, 1800313. [CrossRef]
15. Grosskopf, A.K.; Roth, G.A.; Smith, A.A.; Gale, E.C.; Hernandez, H.L.; Appel, E.A. Injectable supramolecular polymer–nanoparticle hydrogels enhance human mesenchymal stem cell delivery. *Bioeng. Transl. Med.* **2020**, *5*, e10147. [CrossRef]
16. Lyu, Y.; Azevedo, H.S. Supramolecular hydrogels for protein delivery in tissue engineering. *Molecules* **2021**, *26*, 873. [CrossRef]
17. Dankers, P.Y.; van Luyn, M.J.; Huizinga-van der Vlag, A.; van Gemert, G.M.; Petersen, A.H.; Meijer, E.; Janssen, H.M.; Bosman, A.W.; Popa, E.R. Development and in-vivo characterization of supramolecular hydrogels for intrarenal drug delivery. *Biomaterials* **2012**, *33*, 5144–5155. [CrossRef] [PubMed]
18. Raymond, D.M.; Abraham, B.L.; Fujita, T.; Watrous, M.J.; Toriki, E.S.; Takano, T.; Nilsson, B.L. Low-molecular-weight supramolecular hydrogels for sustained and localized in vivo drug delivery. *ACS Appl. Bio Mater.* **2019**, *2*, 2116–2124. [CrossRef] [PubMed]
19. Eivazzadeh-Keihan, R.; Noruzi, E.B.; Aliabadi, H.A.M.; Sheikhaleslami, S.; Akbarzadeh, A.R.; Hashemi, S.M.; Gorab, M.G.; Maleki, A.; Cohan, R.A.; Mahdavi, M.; et al. Recent advances on biomedical applications of pectin-containing biomaterials. *Int. J. Biol. Macromol.* **2022**, *217*, 1–18. [CrossRef] [PubMed]
20. Minzanova, S.T.; Mironov, V.F.; Arkhipova, D.M.; Khabibullina, A.V.; Mironova, L.G.; Zakirova, Y.M.; Milyukov, V.A. Biological Activity and Pharmacological Application of Pectic Polysaccharides: A Review. *Polymers* **2018**, *10*, 1407. [CrossRef]
21. Suner, S.S.; Ari, B.; Sutekin, S.D.; Sahiner, N. Biocompatible poly (galacturonic acid) micro/nanogels with controllable degradation via tunable chemical crosslinking. *Int. J. Biol. Macromol.* **2022**, *201*, 351–363. [CrossRef]
22. Wasupalli, G.K.; Verma, D. Development of chitosan-polygalacturonic acid polyelectrolyte complex fibrous scaffolds using the hydrothermal treatment for bone tissue engineering. *J. Biomed. Mater. Res. Part A* **2023**, *111*, 354–366. [CrossRef]
23. Sikkema, R.; Zhang, C.; Zhitomirsky, I. New developments in synthesis of bioceramics, electrophoretic deposition of biopolymer, and composites using organic bases. *Colloids Surf. A Physicochem. Eng. Asp.* **2025**, *716*, 136691. [CrossRef]
24. Clifford, A.; D'Elia, A.; Deering, J.; Lee, B.E.J.; Grandfield, K.; Zhitomirsky, I. Electrochemical Fabrication and Characterization of Pectin Hydrogel Composite Materials for Bone Tissue Repair. *ACS Appl. Polym. Mater.* **2020**, *2*, 3390–3396. [CrossRef]
25. Iviglia, G.; Cassinelli, C.; Torre, E.; Baino, F.; Morra, M.; Vitale-Brovarone, C. Novel bioceramic-reinforced hydrogel for alveolar bone regeneration. *Acta Biomater.* **2016**, *44*, 97–109. [CrossRef]
26. Wasupalli, G.K.; Verma, D. Thermosensitive injectable hydrogel based on chitosan-polygalacturonic acid polyelectrolyte complexes for bone tissue engineering. *Carbohydr. Polym.* **2022**, *294*, 119769. [CrossRef]
27. Lin, C.-Y.; Peng, H.-H.; Chen, M.-H.; Sun, J.-S.; Chang, C.-J.; Liu, T.-Y.; Chen, M.-H. Ibuprofen-conjugated hyaluronate/polygalacturonic acid hydrogel for the prevention of epidural fibrosis. *J. Biomater. Appl.* **2016**, *30*, 1589–1600. [CrossRef] [PubMed]
28. Wang, D.; Wang, W.; Wang, P.; Wang, C.; Niu, J.; Liu, Y.; Chen, Y. Research progress of colon-targeted oral hydrogel system based on natural polysaccharides. *Int. J. Pharm.* **2023**, *643*, 123222. [CrossRef]
29. Finney, R.; Somers, G. The anti-inflammatory activity of glycyrrhetinic acid and derivatives. *J. Pharm. Pharmacol.* **1958**, *10*, 613–620. [CrossRef] [PubMed]
30. Richard, S.A. Exploring the pivotal immunomodulatory and anti-inflammatory potentials of glycyrrhizic and glycyrrhetinic acids. *Mediat. Inflamm.* **2021**, *2021*, 6699560. [CrossRef] [PubMed]
31. Zhang, D.; Liu, Y.; Wang, M.; Lyu, H.; Sun, Y. The antitumor mechanism of glycyrrhetinic acid and its applications in cancer treatment. *Med. Oncol.* **2025**, *42*, 331. [CrossRef] [PubMed]
32. Pang, X.; Zhitomirsky, I. Electrodeposition of composite hydroxyapatite–chitosan films. *Mater. Chem. Phys.* **2005**, *94*, 245–251. [CrossRef]
33. He, Q.; Kobayashi, K.; Kusumi, R.; Kimura, S.; Enomoto, Y.; Yoshida, M.; Kim, U.-J.; Wada, M. In Vitro Synthesis of Branchless Linear (1 → 6)-α-d-Glucan by Glucosyltransferase K: Mechanical and Swelling Properties of Its Hydrogels Crosslinked with Diglycidyl Ethers. *ACS Omega* **2020**, *5*, 31272–31280. [CrossRef]
34. Cassimiro, D.L.; Ribeiro, C.A.; Capela, J.M.; Crespi, M.S.; Capela, M.V. Kinetic parameters for thermal decomposition of supramolecular polymers derived from flunixin-meglumine adducts. *J. Therm. Anal. Calorim.* **2011**, *105*, 405–410. [CrossRef]
35. Rundfeldt, C.; Klein, P.; Boison, D.; Rotenberg, A.; D'Ambrosio, R.; Eastman, C.; Purnell, B.; Murugan, M.; Goodkin, H.P.; Löscher, W. Preclinical pharmacokinetics and tolerability of a novel meglumine-based parenteral solution of topiramate and topiramate combinations for treatment of status epilepticus. *Epilepsia* **2023**, *64*, 888–899. [CrossRef] [PubMed]
36. Cassimiro, D.L.; Ferreira, L.M.; de Souza, A.L.R.; Fonseca, M.; Kurokawa, S.S.; Alonso, J.D.; Sarmento, V.H.V.; Ribeiro, C.A. On the influence of fatty acid chain unsaturation on supramolecular gelation of aminocarbohydrate-based supra-amphiphiles. *J. Therm. Anal. Calorim.* **2018**, *134*, 1599–1609. [CrossRef]
37. Rojek, B.; Wesolowski, M. FTIR and TG analyses coupled with factor analysis in a compatibility study of acetazolamide with excipients. *Spectrochim. Acta Part A Mol. Biomol. Spectrosc.* **2019**, *208*, 285–293. [CrossRef]

38. Lu, Y.; Miller, J.D. Carboxyl stretching vibrations of spontaneously adsorbed and LB-transferred calcium carboxylates as determined by FTIR internal reflection spectroscopy. *J. Colloid Interface Sci.* **2002**, *256*, 41–52. [CrossRef]
39. Said, N.S.; Olawuyi, I.F.; Lee, W.Y. Pectin hydrogels: Gel-forming behaviors, mechanisms, and food applications. *Gels* **2023**, *9*, 732. [CrossRef] [PubMed]
40. Quan, W.; Kong, S.; Ouyang, Q.; Tao, J.; Lu, S.; Huang, Y.; Li, S.; Luo, H. Use of 18β-glycyrrhetinic acid nanocrystals to enhance anti-inflammatory activity by improving topical delivery. *Colloids Surf. B Biointerfaces* **2021**, *205*, 111791. [CrossRef] [PubMed]
41. Dong, L.; Mai, Y.; Liu, Q.; Zhang, W.; Yang, J. Mechanism and improved dissolution of glycyrrhetinic acid solid dispersion by alkalizers. *Pharmaceutics* **2020**, *12*, 82. [CrossRef]
42. Coleman, M.M.; Skrovanek, D.J.; Hu, J.; Painter, P.C. Hydrogen bonding in polymer blends. 1. FTIR studies of urethane-ether blends. *Macromolecules* **1988**, *21*, 59–65. [CrossRef]
43. Kumar, K.S.; Bindu, M.; Suresh, S.; Anil, A.; Sujoy, S.; Mohanan, A.; Periyat, P. Investigation on swelling behavior of sodium alginate/black titania nanocomposite hydrogels and effect of synthesis conditions on water uptake. *Results Eng.* **2023**, *20*, 101460. [CrossRef]
44. Hendy, J.M.; Mansour, M.S.; Abdel-Megeed, A.; Al-Oufy, A.K.; Salem, M.Z. Swelling Properties of Superabsorbent Hydrogels Based on Carboxymethyl Cellulose With Silica, Kaolin, and Bentonite Particles for Agricultural Applications. *ChemistrySelect* **2025**, *10*, e04489. [CrossRef]
45. Feng, W.; Wang, Z. Tailoring the swelling-shrinkable behavior of hydrogels for biomedical applications. *Adv. Sci.* **2023**, *10*, 2303326. [CrossRef]
46. Dawn, A.; Kumari, H. Low molecular weight supramolecular gels under shear: Rheology as the tool for elucidating structure–function correlation. *Chem.-A Eur. J.* **2018**, *24*, 762–776. [CrossRef] [PubMed]
47. Cordier, P.; Tournilhac, F.; Soulié-Ziakovic, C.; Leibler, L. Self-healing and thermoreversible rubber from supramolecular assembly. *Nature* **2008**, *451*, 977–980. [CrossRef]
48. Wang, R.; Hao, X.; Yang, H. Using a solvent-induced self-assembly approach to fabricate and tune the organogels and hydrogels. *Colloid Polym. Sci.* **2024**, *302*, 163–171. [CrossRef]

Disclaimer/Publisher's Note: The statements, opinions and data contained in all publications are solely those of the individual author(s) and contributor(s) and not of MDPI and/or the editor(s). MDPI and/or the editor(s) disclaim responsibility for any injury to people or property resulting from any ideas, methods, instructions or products referred to in the content.